ELSEVIER

Ceramics International 29 (2003) 513–518

CERAMICS INTERNATIONAL

www.elsevier.com/locate/ceramint

Thermal behaviour of alumina precursor obtained by the aluminium sulphate–urea reaction in boiling aqueous solution

K. Ada[a], Y. Sarıkaya[b,*], T. Alemdaroğlu[b], M. Önal[b]

[a]*Department of Chemistry, Kırıkkale University, Faculty of Science and Literature, Kırıkkale, Turkey*
[b]*Department of Chemistry, Tandoğan, Ankara University, Faculty of Sciences, 06100 Ankara, Turkey*

Received 8 April 2002; received in revised form 14 September 2002; accepted 4 October 2002

Abstract

An aqueous solution containing 0.1 M Al^{3+} and excess urea was boiled for 4 h to obtain an alumina precursor precipitate. The precursor precipitate was separated into several portions and each portion was heated at a different temperature for 4 h between 100–1100 °C. Thermally treated samples were investigated by X-ray diffraction (XRD) analysis, differential thermal analysis (DTA), thermogravimetric analysis (TGA) and scanning electron microscopy (SEM) techniques. The particle size distributions (PSD) and nitrogen adsorption–desorption isotherms at 77 K of the same samples were also determined. The XRD data showed that the previously amorphous precursor was transformed respectively into δ-Al_2O_3 at 850 °C and α-Al_2O_3 at 1100 °C. The TGA data were used to calculate the activation energies for the dehydration and dehydroxylation of the precursor according to the Coats–Redfern equation and the results were discussed. From the SEM and PSD data, it was determined that most of the precursor particles were agglomerated. The adsorption data were used to calculate the specific surface areas (A) and the desorption data were used to calculate the specific micropore–mesopore volumes (V). At 100 °C, the A and V values were respectively, 15 $m^2\ g^{-1}$ and 0.030 $cm^3\ g^{-1}$. They increased by increasing temperature and reached their maximum values of 117 $m^2\ g^{-1}$ and 0.350 $cm^3\ g^{-1}$ respectively at 900 °C and then decreased promptly at 1000 °C.

Keywords: B. Porosity; C. Thermal properies; D. Al_2O_3; Dehydration; Dehydroxylation

1. Introduction

Alumina powders are extensively used in the production of ceramics, abrasives, medications, membranes, chromatographic column support materials, adsorbents and catalysts [1,2]. New procedures besides the conventional Bayer procedure were developed to produce alumina precursors possessing different characteristics required by different application areas [3–5]. The production of powders having specific crystal sizes, crystal shapes, particle shapes, particle sizes, agglomeration degrees and porosities is possible if the precursors obtained by these methods are used [6–13]. Some of these non-conventional methods may be mentioned as hydrothermal synthesis [14], microwave synthesis [15], emulsion evaporation [16–18] and chemical precipitation from solution [19].

Heterogeneous precipitation takes place if the reactants are in different phases during precipitation and the above mentioned properties of the precursor cannot be controlled. A homogeneous precipitation in which the reactants are in the same phase has to be made in order to control these properties. The homogeneous precipitation of alumina precursors is carried out by heating the aqueous solution containing excess urea and an aluminium salt approximately up to its boiling temperature [20,21]. Alumina powders are then obtained by the calcination of the precursor precipitates at 1000 °C. It was determined that the concentration of Al^{3+} in the heated aqueous solution during precipitation affected the properties of the resultant alumina powders. For example, as the concentration of Al^{3+} in the heated aqueous solution increased, the agglomeration degrees of the alumina powders increased whereas their porosities decreased [22]. Aim of this study was to investigate

* Corresponding author. Tel.: +90-312-212-67-20-1164; fax: +90-312-223-23-95.
E-mail address: sakaya@science.ankara.edu.tr (Y. Sarıkaya).

0272-8842/03/$30.00
PII: S0272-8842(02)00195-5

some of the physicochemical properties such as crystallinity, dehydration, dehydroxylation, particle size distribution, specific surface area and specific pore volume of these thermally treated precursors.

2. Experiments

$Al_2(SO_4)_3.18H_2O$, $CO(NH_2)_2$, 65% HNO_3 (1.40 g cm^{-3}) and 25% NH_3 (0.91 g cm^{-3}) (all analytical grade from Merck Company) were used. A 0.4 M $Al_2(SO_4)_3$ stock aqueous solution was prepared by $Al_2(SO_4)_3.18H_2O$. Since this salt is not very soluble, a small amount of 0.1M HNO_3 was added to help its dissolution during the peparation of the stock solution.

As a first step for the preparation of aqueous solutions with desired aluminium sulphate–urea concentrations, a preliminary study was realized to assure a quantitative reaction between urea and aluminium sulphate. It was determined that a ratio of [urea]/$[Al^{3+}]\approx 5.4$ fullfilled this condition. The stock $Al_2(SO_4)_3$ solution and solid urea were used to prepare a homogeneous solution (0.8 dm^3) that satisfied the earlier ratio. The pH value necessary for the precipitation of the alumina precursor from a solution whose $[Al^{3+}]=0.1$ M was calculated [22] as pH = 3.42 by using the ionization constant of water ($K_w=10^{-14}$) and the solubility product constant of $Al(OH)_3$ that is assumed to be approximately invariable by temperature ($K_{sp}=1.9\times10^{-33}$). Since the stock solution was rather acidic due to the added HNO_3, dilute NH_3 solution was added drop by drop to adjust the pH of the solution to the calculated value. The solution hence prepared was stirred continuously with a magnetic stirrer and heated up to its boiling temperature and continued boiling for 4 h for complete precipitation of the precursor. The precipitation process was repeated several times until sufficient amount of precursor was obtained. The precursors were separated by filtration and were first washed with distilled water and then with acetone until they were free of SO_4^{2-} and NO_3^- ions and urea. The precursor precipitate was separated into several portions and one portion was heated for 4 hours at 100 °C and a stock precursor powder was obtained. Three different precursor powders were also prepared by heating the other portions respectively for 24, 48 and 78 h. Ten samples were taken from the stock precursor powder and each was heated at a different temperature between 200 and 1100 °C. The thermally treated precursor powders were coded respectively as A100, A200,..., A1100. The static mass loss during thermal treatments was recorded by mass measurements before and after thermal treatments.

The X-ray diffraction patterns of the thermally treated precursor powders were recorded by a Rikagu D-max 2200 Powder Diffractometer with a Ni filter and CuK_α X-rays having 0.15418 nm wavelength. The differential thermal analysis (DTA) and thermogravimetric analysis (TGA) curves of the A100 sample were recorded by a Netzch instrument (Simultaneous TG–DTG–DTA Instrument model 229) at a heating rate of 20 K min^{-1}. Calcined kaolin was used as an inert material. An electron microscope (LEO 435) was used to take SEM view of the thermally treated precursor powders. The specific outer surface areas (S), i.e. apparent geometric areas and particle size distributions (PSD) of the same powders were determined by a Mastersizer Instrument (Malvern Instruments, model Micron) based on a light scattering technique. The adsorption and desorption of nitrogen on the thermally treated precursor powders, at liquid nitrogen temperature were investigated by a volumetric adsorption instrument. The instrument was constructed completely of pyrex glass and connected to high vacuum [23].

3. Results and discussion

3.1. XRD Data

The XRD patterns of A100, A850 and A1100 samples are shown in Fig. 1. From the XRD patterns not given here, it was observed that some of the wide peaks seen in the XRD patterns of the A100 sample widened as the heating period increased up to around 72 h. Similar widenings were also observed as the heating temperature increased up to 600 °C. It was perceived that none

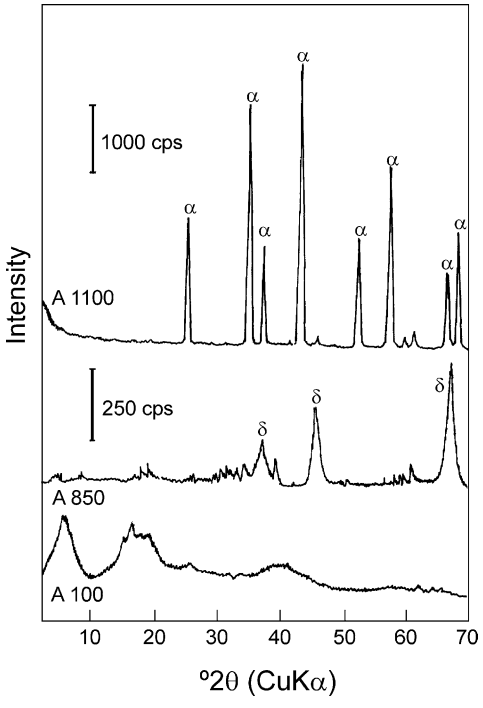

Fig. 1. The XRD patterns of the A100, A850 and A1100 samples.

of these peaks were characteristic of any alumina phase. Hence, it was decided that the precursor powders were amorphous in nature up to 600 °C. Inspection of the XRD patterns indicated that crystallization of the precursor powders began at 600 °C and a crystal alumina phase [24] appeared at 850 °C (Fig. 1) Although most of the characteristic peaks of θ-Al_2O_3 and δ-Al_2O_3 overlapped, considering the peak positions and peak intensities [25] of the A850 sample it was decided that the present phase was δ-Al_2O_3. Examination of the other XRD patterns not given here showed that no important change of the crystal structure has occurred up to 1100 °C. At this temperature, α-Al_2O_3 was formed (Fig. 1).

3.2. DTA and TGA data

The DTA and TGA curves of the A100 sample are shown in Fig. 2. The endothermic peak between 20 °C and 500 °C on the DTA curve was due to the elimination of water in the sample. The fact that this peak contained a minimum (a) at 155 °C and a shoulder (b) at 260 °C gave the impression that there were two types of interaction between water and the amorphous solid phase. The TGA curve showed that around 30% (expressed as mass per cent) water was lost during dehydration. Water was lost (3%) between 500 and 800 °C. Since partial dehydroxylation took place in this interval, it appeared that crystallization began at this temperature interval. It was decided that the endothermic peak which appeared between 800 and 1100 °C was due to dehydroxylation since δ-Al_2O_3 was formed in this interval. It was determined that the mass% of lost water in this interval was 15% and the mass loss was negligible between 950 and 1100 °C.

The dynamic decomposition fractions (α) were calculated by taking the ratios of mass loss at each temperature to the maximum mass loss at 1100 °C. Similarly the static α values were calculated by using the mass measurements before and after thermal treatments. The curves (α–T) that show the variations of the dynamic and static decomposition fractions as a function of temperature are given in Fig. 3. Although these two curves did not exactly coincide with eachother, a good correlation between the two was observed at each point. In the dynamic α–T curve, the sections a and b show respectively, the first and second dehydrations and section c shows the dehydroxylation.

The Coats–Redfern equation [26,27] can be given as follows for physical or chemical deformations of the, solid(1)→solid(2)+gas, type that are assumed to occur by first order chemical reaction kinetics

$$\ln\{[-\ln(1-\alpha)]/T^2\} = -E/RT + \ln[(AR/\beta E)(1-2RT/E)] \quad (1)$$

where T is the average deformation temperature, $\beta = dT/dt$ is the heating rate, E is the activation energy of deformation, R is the universal gas constant and $\ln[(AR/\beta E)(1-2RT/E)]$ is a quantity that stays nearly constant. The Coats−Redfern straight lines of the a, b and c deformations which were obtained by the TGA data [28,29] are shown in Fig. 4. The activation energies were respectively calculated as $E_a = 15$ kJ mol^{-1}, $E_b = 11$ kJ mol^{-1} and $E_c = 156$ kJ mol^{-1}, from the slopes of these straight lines. The fact that E_c was considerably larger than E_b and E_a showed that the different dehydrations were physical events whereas the dehydroxylation was a chemical event. The presence of two dehydrations that have different activation energies gives the impression that the prepared precursor was a pseudoboehmite [30].

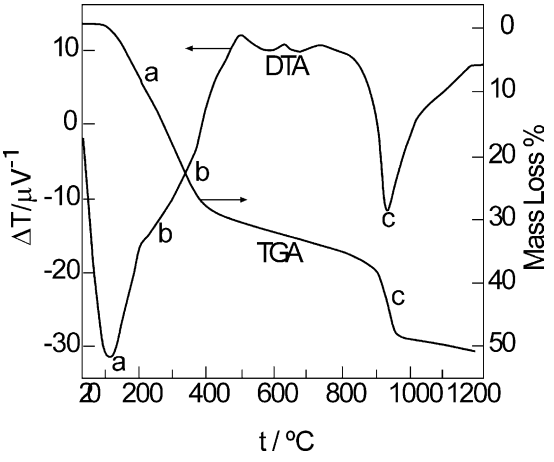

Fig. 2. The DTA and TGA curves of the A100 sample (a and b: dehydration, c: dehydroxylation).

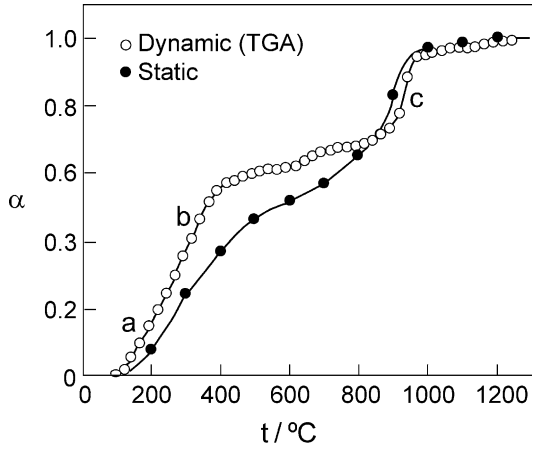

Fig. 3. The variations of the dynamic decomposition factor calculated by using the TGA data and the static decomposition factor calculated by using the weight measurements as a function of thermal treatment temperature.

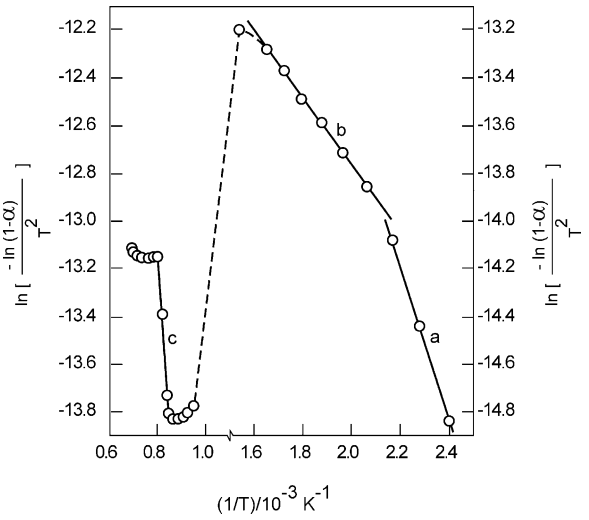

Fig. 4. The Coats–Redfern straight lines plotted by using the TGA data.

3.3. SEM and PSD Data

The SEM photographs of the A100 and A900 samples are given in Fig. 5. It was clearly observed from these photographs that the precursor powder particles were spherical, some of these unequally sized spherical particles

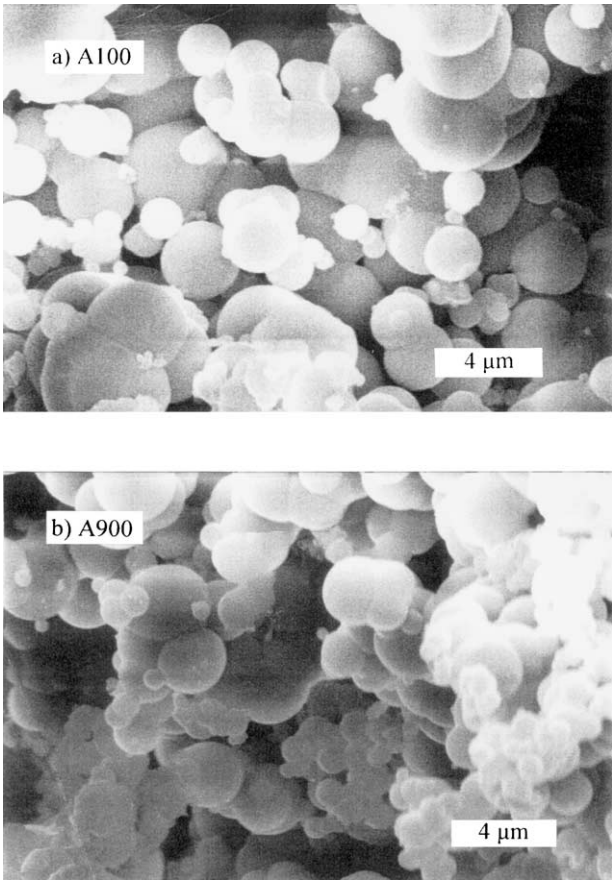

Fig. 5. The SEM photographs of the A100 and A900 samples.

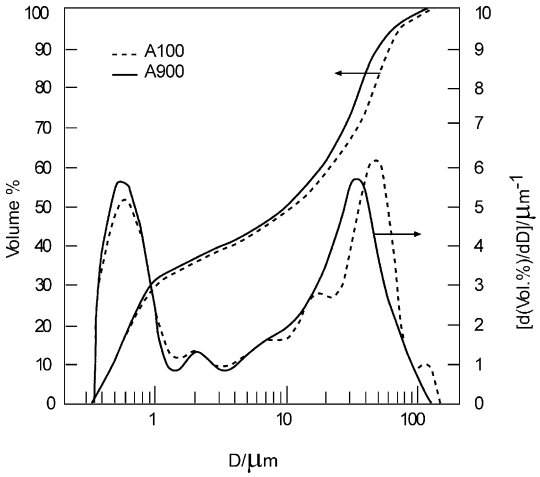

Fig. 6. The PSD curves of the A100 and A900 samples.

were agglomerated and considerable morphological transformation did not occur during thermal treatments.

The PSD curves of the A100 and A900 samples are given in Fig. 6. The good correlation of these PSD curves showed that the change in particle sizes was negligible. The evaluation of the SEM and PSD data alltogether showed that the sizes of independent particles changed between 0.35 and 7 μm and those of the agglomerated ones changed between 7 and 120 μm. The agglomeration degree was estimated as 60% from the PSD curves.

3.4. Adsorption and desorption data

The adsorption and desorption isotherms at liquid nitrogen temperature of the A100, A700 and A900 samples are given in Fig. 7. Here, p shows the equilibrium pressure of adsorption, p^0 shows the vapor pressure of

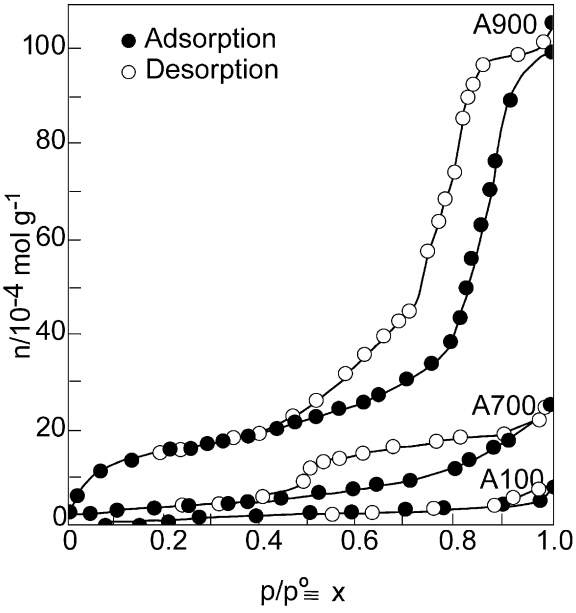

Fig. 7. The adsorption and desorption isotherms of nitrogen on the A100, A700 and A900 samples at liquid nitrogen temperature.

liquid nitrogen and $p/p^0 = x$ shows the relative equilibrium pressure, n represents the adsorption capacity defined as the amount of nitrogen adsorbed on one gram of solid at any relative equilibrium pressure. The adsorption capacity that was very small in the A100 sample increased as the thermal treatment temperature increased and reached its maximum value at 900 °C and then decreased at higher temperatures.

The specific surface areas (A) of the samples were determined by using the adsorption data at the relative equilibrium pressure interval of $0.05 < x < 0.35$ according to the standard Brunauer, Emmet and Teller (BET) procedure [31]. The variation of A as a function of thermal treatment temperature is given in Fig. 8. It was observed that the A values increased by increasing temperature, reached a maximum at 900 °C and then decreased suddenly at higher temperatures, and that the S values measured by the light scattering of particles were very small compared to A values. For example when the value of A was 116 $m^2\ g^{-1}$, the value of S was 4 $m^2\ g^{-1}$. Fig. 7 shows that at around $x \approx 0.95$ the adsorption and desorption isotherms coincide. During adsorption, when $0 < x < 0.35$, first the micropores that are assumed to be cylindrical and whose radii (r) are smaller than 1 nm, are filled by monomolecular adsorption then, the inner surfaces of the mesopores whose radii lie within the interval 1 nm $< r <$ 25 nm are covered by multimolecular adsorption. As x increases, first the smaller then the larger mesopores whose walls are multimolecularly covered are filled successively by capillary condensation. When the relative equilibrium pressure reaches to the value of $x = 1$, bulk condensation takes place. The larger and smaller mesopores that were filled during adsorption are evacuated successively during desorption as the relative equilibrium pressure decreased in the interval $1 < x < 0.35$. The relative equilibrium pressure at which the largest mesopore ($r = 25$ nm) begins to evacuate was calculated by the Kelvin equation [32] to be $x = 0.96$. The n values corresponding to the value of x at which all of the micropores and mesopores were full were read on the desorption isotherms. These adsorption capacities were expressed in terms of liquid nitrogen volumes and were taken as specific micropore-mesopore volumes (V) [33,34]. The variation of V as a function of thermal treatment temperature is represented in Fig. 8. V and A show a parallel variation. From the observed dehydrations at temperatures between 100 and 500 °C, it was understood that the pore structure of the precursor powder was not notably affected. Porosity developed rapidly at 600 °C where the crystallization began and reached a maximum at around 900 °C where the dehydroxylation was completed and δ-Al_2O_3 was formed. The porosity decreased at above 900 °C. It was thought that this decrease was due to inter particle sintering, closing of the micropores and shrinkage of the mesopores.

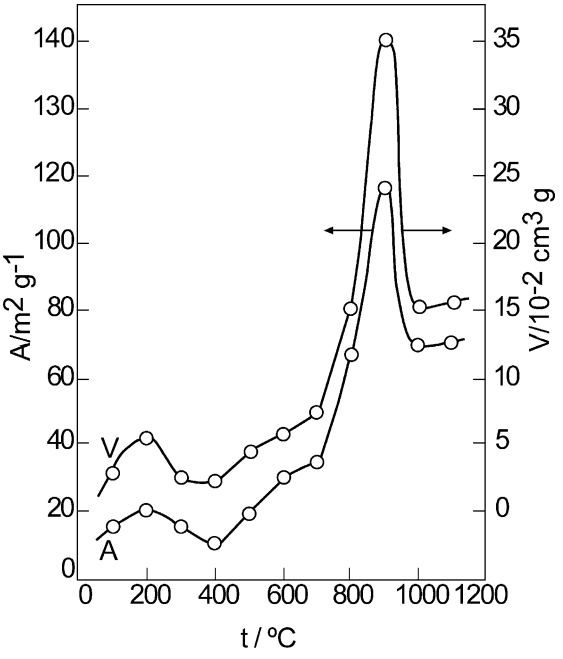

Fig. 8. The variations of the specific surface area (A) and specific pore volume (V) as a function of thermal treatment temperature.

4. Conclusion

In this study, it was observed that the homogeneous precipitation of alumina precursor from a boiling aqueous solution of aluminium sulphate and urea produced mostly agglomerated and spherical particles. It was also observed that the thermal treatment of the alumina precursor did not cause a change in particles shape and size. Considering the activation energies, it was demonstrated that the dehydration of the amorphous precursor was a physical decomposition whereas the dehydroxylation was a chemical decomposition. Dehydroxylation and crystallization began at the same temperature. Formation of phases other than δ-Al_2O_3 and α-Al_2O_3 was not observed during the thermal treatment of the precursor. On the other hand, the thermal treatment of alumina precursors at various temperatures between 100 and 1100 °C produced alumina powders that have various degrees of porosity. Hence, it was concluded that the preparation of alumina powders possessing specific porosities would be possible by applying thermal treatments to precursors obtained by the aluminium sulphate–urea reaction.

Acknowledgements

The authors thank the Ankara University Research Fund for funding this work by the project 96-25-00-18.

References

[1] W.H. Gitzen, Alumina as a Ceramic Material, The American Ceramic Society, Columbus, OH, 1970.

[2] E. Dorre, H. Hubner, B. Ilschner, N.J. Grand, Alumina: Processing, Properties and Applications, Springer, Berlin, 1984.

[3] B.C. Cornilsen, J.S. Reed, Homogeneous precipitation of basic aluminium salts as precursors for alumina, American Ceramic Society Bulletin 58 (12) (1979) 1199.

[4] D.W. Johnson Jr., Nonconventional powder preparation techniques, Ceramic Bulletin 60 (2) (1981) 221–224.

[5] J.E. Blendell, H.K. Bowen, R.L. Coble, High purity alumina by controlled precipitation from aluminium sulfate solutions, American Ceramic Society Bulletin 63 (6) (1984) 797.

[6] P. Hugo, H. Koch, Production of porous alumina with defined bimodal pore structure, German Chemical Engineering 2 (1979) 24–30.

[7] F.W. Dynys, J.W. Halloran, Compaction of aggregated alumina powder, Journal of American Ceramic Society 66 (9) (1983) 655–659.

[8] R.F. Vogel, G. Marcelin, W.L. Kehl, The preparation of controlled pore alumina, Applied Catalysis 12 (1984) 237–248.

[9] D.L. Trimm, A. Stainslaus, The control of pore size in alumina catalyst supports: a review, Applied Catalysis 21 (1986) 215–238.

[10] P. Vincenzini (Ed.), Ceramic Powders, Elsevier, Amsterdam, 1983.

[11] G.H. Maher, C.E. Hutchins, S.D. Ross, Preparation and characterization of ceramic fine powders produced by the emulsion process, American Ceramic Society Bulletin 72 (5) (1993) 72–76.

[12] D. Sordelet, M. Akınc, Preparation of spherical, monosized Y_2O_3 precursor particles, Journal of Colloid and Interface Science 122 (1) (1988) 47–59.

[13] K. Hellgart, D. Chadwick, Effect of pH of precipitation on the preparation of high surface area aluminas from nitrate solutions, Industrial and Engineering Chemistry Research 37 (2) (1998) 405–411.

[14] W.J. Dowson, Hydrothermal synthesis of advanced ceramic powders, American Ceramic Society Bulletin 67 (10) (1988) 1673–1678.

[15] S.G. Deng, Y.S. Lin, Microwave synthesis of mesoporous and microporous alumina powders, Journal of Materials Science Letters 16 (1997) 1291–1294.

[16] Y. Sarıkaya, M. Akınc, Preparation of alumina microshells by emulsion evaporation technique, Ceramics International 14 (1988) 239–244.

[17] İ. Sevinc, Y. Sarıkaya, M. Akınc, Adsorption characteristics of alumina powders produced by emulsion evaporation, Ceramics International 17 (1991) 1–4.

[18] Y. Sarıkaya, T. Alemdaroglu, M. Onal, Determination of the shape, size and porosity of fine α-Al_2O_3 powders prepared by emulsion evaporation, Journal of the European Ceramic Society 22 (2002) 305–309.

[19] P.L. Chen, I.W. Chen, Reactive cerium (IV) oxide powders by the homogeneous precipitation method, Journal of the American Ceramic Society 76 (6) (1993) 1577–1583.

[20] S. Ramanathan, S.K. Roy, R. Bhat, D.D. Upadhyaya, A.R. Biswas, Preparation and characterization of boehmite precursor and sinterable alumina powder from aqueous aluminium chloride–urea reaction, Journal of Alloys and Compounds 243 (1996) 39–44.

[21] S. Ramanathan, S.K. Roy, R. Bhat, D.D. Upadhyaya, A.R. Biswas, Alumina powders from aluminium nitrate–urea and aluminium sulphate–urea reactions—the role of the precursor anion and process conditions on characteristics, Ceramics International 23 (1997) 45–53.

[22] Y. Sarıkaya, K. Ada, T. Alemdarodlu, İ Bozdodan, The effect of Al^{3+} concentration on some physicochemical properties of alumina powders which were obtained by the reaction of aluminium sulphate and urea in boiling aqueous solution, Journal of the European Ceramic Society 22 (2002) 1905–1910.

[23] Y. Sarıkaya, S. Aybar, The adsorption of NH_3, N_2O and CO_2 gases on the 5A molecular sieve, Communications (Faculty of Science, University of Ankara) B24 (1978) 33–39.

[24] G.B. Leonard (Ed.), Powder Diffraction File, Sets 6-10, Inorganic Volume No: RB119, Joint Committee on Powder Diffraction Standards, Philadelphia, 1964.

[25] B.C. Lippens, J.J. Steggerda, Active Alumina, in: J.H. De Boer, B.G. Linsen (Eds.), Physical and Chemical Aspects of Adsorbents and Catalysts, Academic Press, London, 1970, pp. 171–211.

[26] A.W. Coats, J.P. Redfern, Kinetic parameters from thermogravimetric data, Nature 201 (1964) 68–69.

[27] C. Güler, N. Sarıer, Kinetics of the thermal dehydration of acid activated montmorillonite by the rising temperature technique, Thermochimica Acta 159 (1990) 29–33.

[28] Y. Sarıkaya, M. Onal, B. Baran, T. Alemdarodlu, The effect of thermal treatment on some of the physicochemical properties of a bentonite, Clays and Clay Minerals 48 (2000) 557–562.

[29] Y. Sarıkaya, İ. Svinc, M. Akınc, The effect of calcination temperature on some of the adsorptive properties of fine alumina powders produced by emulsion evaporation, Powder Technology 116 (2001) 109–114.

[30] B.R. Baker, R.M. Pearson, Water content of pseudoboehmite: a new model for its structure, Journal of Catalysis 33 (1974) 265–278.

[31] S. Brunauer, P.H. Emmett, E. Teller, Adsorption of gases in multimolecular layers, Journal of the American Chemical Society 60 (1938) 309–319.

[32] S.S. Gregg, K.S.W. Sing, Adsorption, Surface Area and Porosity, Academic Press, London, 1992.

[33] M. Onal, Y. Sarıkaya, T. Alemdarodlu, The investigation of the icroporous and mesoporous structures of the Re-adiye (Tokat/Turkey) bentonite and its fractions, Turkish Journal of Chemistry 25 (2001) 241–249.

[34] Y. Sarıkaya, İ. Sevinc, M. Onal, T. Alemdarodlu, Determination of some of the physicochemical properties of fine alumina powders prepared by emulsion evaporation, Turkish Journal of Chemistry 25 (2001) 283–291.